Chemical Engineering Science, 1975, Vol. 30, pp. 1341-1351. Pergamon Press. Printed in Great Britain

CATALYST POISONING AND FIXED BED REACTOR DYNAMICS

H. S. WENG†, G. EIGENBERGER‡ and J. B. BUTT§
Department of Chemical Engineering and Ipatieff Catalytic Laboratory, Northwestern University, Evanston, IL 60201, U.S.A.

(Received 25 January 1975; accepted 16 April 1975)

Abstract—The poisoning kinetics of thiophene on Ni-kieselguhr catalysts and the deactivation behavior of nonisothermal fixed bed reactors have been studied experimentally using benzene hydrogenation as a model exothermic reaction. The time dependent axial temperature profiles in the reactors were measured and compared with values evaluated from a dispersion model, the parameters of which have been determined in separate experimentation.

Poisoning kinetics were measured in a series of differential reactor experiments at atmospheric total pressure, thiophene partial pressures of 0·037–0·19 torr, hydrogen to benzene molar ratios >8/1 and temperatures from 60–180°C. Excellent agreement was found with a power law equation for the rate of change of activity with time, first order in catalyst activity and in thiophene concentration, with an experimental activation energy of 1080 kcal/kmole.

This correlation of poisoning kinetics, however, was not able to predict the propagation of the zone of activity (hot-spot) on poisoning of an integral fixed bed reactor. Initial (steady state) temperature profiles were modeled satisfactorally, but the rate of migration of the hot spot was found experimentally to be more rapid than that predicted from the correlation of poisoning kinetics. A semi-empirical two site deactivation model is shown to resolve the discrepancy.

INTRODUCTION

The problem of catalyst deactivation in fixed bed reactors is widely encountered in processing applications, yet relatively few studies, particularly those giving experimental results, have been reported in the literature. The bulk of results both theoretical and experimental, have been summarized in a recent review by Butt[1]. Eberly *et al.*[2] conducted a study of coke formation for cumene cracking in a fixed bed of silica–alumina catalyst. They found that coke formation was a complex function of the length of the cracking cycle and space velocity. Menon and Sreeramamurthy[3] and Menon *et al.*[4] have measured the time dependence of temperature profile and reaction rate in a fixed bed of charcoal catalyst used for the air oxidation of H_2S. No quantitative interpretation of these results have been presented. Kunigita *et al.*[5] have reported the results of a systematic investigation of coke formation in fixed bed reactors. The experimental system was dehydrogenation of n-butane over alumina–chromia catalysts; they analyzed coke formation effects on the overall efficiency of fixed bed processing using an analog computer technique.

Recent experimental studies are represented by the work of Lambrecht *et al.*[6] who investigated the coking of a platinum reforming catalyst in the isomerization of n-pentane. They evaluated the parameters appearing in the deactivation model of Froment and Bischoff[7] by fitting experimental conversion-time variation and coke profiles with both differential and integral methods. Pexidr *et al.*[8] measured the axial concentration and temperature profiles in a non-isothermal, non-adiabatic pilot plant reactor during the deactivation of a Ni catalyst by CS_2 in benzene hydrogenation, which is the reaction used here. However, they did not attempt to model the transient behavior of the reactor under deactivation conditions.

Richardson[9] obtained the activity profiles of an isothermal fixed bed reactor on sulfiding of a Ni-kieselguhr catalyst through the measurement of the relative ferromagnetic properties of sulfided and unsulfided portions of the bed. It was confirmed that sulfiding (with thiophene and a number of other sulfur compounds) kinetics could be explained by the Bohart–Adams[10] theory of wave propagation through fixed beds. As will be seen in the results of this study, such a theory does not appear adequate for non-isothermal reaction systems.

RESEARCH PROBLEM

The main objectives of this research are to obtain further experimental information on the poisoning of fixed bed reactors and to explore the adequacy of simple models to explain the behavior of the reactor in both steady and transient states. The effect of operating parameters on reactor performance are reported for the benzene hydrogenation reaction over Ni-kieselguhr catalyst with thiophene as the catalyst poison.

EXPERIMENTAL

Reactor and flow system

The experimental flow system is shown in Fig. 1. It is similar to that described by Irving and Butt[11] except that the reactor section is a tubular fixed bed and there are two separate inlet systems to permit switching from thiophene-free to thiophene-containing feed. Three major series of experiments were carried out. In the first a small differential reactor was employed to measure kinetics of the benzene hydrogenation and of the poisoning reaction

†Current address: Department of Chemical Engineering, Cheng Kung University, Tainan, Tawain, Republic of China.
‡Current address: Institut für Systemdynamik und Regelungstechnik, Universität Stuttgart, Stuttgart, Germany.
§To whom correspondence should be addressed.

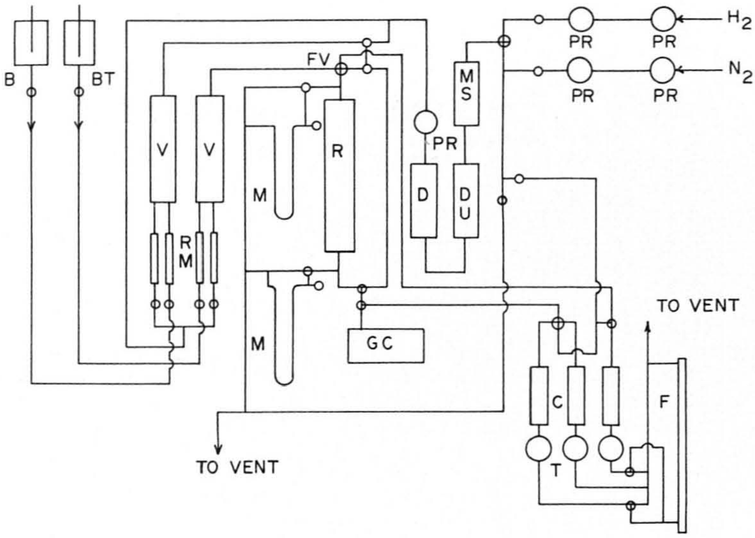

Fig. 1. Schematic of Flow Reactor System. B, Benzene storage; BT, Benzene/thiophene storage; C, Condenser; D, Drier; DU, Deoxo unit; F, Flowmeter; FV, Four-way valve; M, Manometer; MS, Molecular sieve; PR, Pressure regulator; R, Reactor; RM, Rotameter; T, Trap; V, Vaporizer; GC, Gas Chromatograph.

under the experimental conditions of interest; in the second the absorption capacity of the catalyst for thiophene under reaction conditions was determined, also with a tubular fixed bed arrangement. The third series of experiments, to measure reactor transients under poisoning conditions, employed a concentric, double-tubing glass reactor. The inner tube was wound with Nichrome resistance wire and the outer tubing with heating tape. These were used to heat the reactor for catalyst pre-treatment and to initiate reaction at the start of a run. The inner tube was packed in three layers, fore and aft sections of inert glass beads of the same mesh size as the catalyst, and a central section of catalyst diluted 2:1 with glass beads. A 3 mm O.D. thermocouple guide containing a movable iron-constantan thermocouple passed along the entire axis of the reactor. Reactor dimensions and conditions of the deactivation transient experiments are given in Table 1.

Materials

Prepurified grade hydrogen and nitrogen, and high purity grade helium, supplied by Linde, were used in all experiments. All gases were passed through a purification train of 13 X sieve traps for removal of moisture and, in the case of H_2, an Englehard Deoxo unit upstream of a second drier. A.C.S. certified thiophene-free reagent grade benzene, supplied by Fisher Scientific Company, and reagent grade thiophene, supplied by Eastman Organic Chemicals, were used for the liquid feeds. The catalyst was Harshaw Ni-0104T, 58% nickel by weight, crushed to 20/40 or 12/20 U.S. standard mesh for the differential and integral reactor experiments, respectively. Harshaw reports the active nickel surface in the reduced catalyst to be approximately 24 m^2/g. Pyrex glass particles of 12/20 mesh were used to fill the fore and aft reactor sections and for catalyst dilution.

Operation

Catalyst pretreatment consisted of purging the reactor system at room temperature with nitrogen at 1000 cm^3/min for 1 hr, then increasing temperature to 120°C and reducing flow to 200 cm^3/mm for 3 hr. The temperature was then increased to 160°C and hydrogen introduced into the system for 10 hr. This pretreatment was repeated before each series of runs. In the experiments to measure transients of the integral reactor

Table 1. Experimental conditions for fixed bed poisoning runs

Operating Condition / Run:	G1	G2	G3	G4	G5	G7
Total pressure (inlet), torr	750.1	741.7	749.0	741.7	742.7	749.0
Total flow rate, ml/min (sc)	1034.2	1049.6	1551.5	1049.6	1050.4	1554.0
Ambient temp., °C	19.0	23.0	22.0	23.0	23.0	22.0
Inlet temp., °C	45.5	55.0	54.4	45.2	45.5	55.0
Mole fraction C_6H_6	0.028	0.043	0.033	0.043	0.043	0.035
Mole fraction H_2	0.972	0.957	0.967	0.957	0.957	0.965
Thiophene/C_6H_6 x 10^2	1.136	1.136	1.136	1.136	0.565	0.565

All experimental runs with: reactor radius = 0·822 cm; reactor length = 50·00 cm; entrance section length = 14·00 cm; catalyst section length = 9·50 cm; Catalyst wt. = 6·876 gm. Catalyst bulk density = 0·354 g/cm^3; 2:1 (volume) dilution with 12/20 mesh glass beads: 12/20 mesh Ni-0104T.

due to deactivation separate hydrogen flows were introduced into two vaporizers, after catalyst activation, as shown in Fig. 1. One vaporizer was fed with pure benzene while the second was fed a benzene–thiophene mixture of fixed concentration. Initially the pure benzene was fed to the reactor while the thiophene containing feed was directed through an inert bed (not shown in Fig. 1) of the same pressure drop as the reactor. The flow rates of hydrogen and liquid to vaporizer in both feed systems were adjusted to the same values and allowed to stabilize. After the reactor had attained steady state, as indicated by invariance of the temperature profile measured along the axis of the reactor, and inlet and exit concentrations had been measured, the feed was switched to introduce the thiophene-containing mixture into the reactor and the pure benzene feed to the secondary bed. The reactor temperature profile and inlet and exit concentrations were then measured at periodic time intervals.

Analytical

Gas chromatography was used to analyze reactants and products at both the inlet and outlet of the reactor. An F & M 700 laboratory chromatograph with a 12 ft section of $\frac{1}{4}''$ stainless steel column packed with 15% Carbowax (6000) on 80/100 mesh chromosorb *P* was used for benzene/cyclohexane analysis. Operating conditions were those as described by Kehoe[12]. Thiophene concentrations were determined with a Coleman Model 14 Spectrophotometer, using the JIS isatin–sulfuric acid method[13].

RESULTS

Reaction kinetics

The benzene hydrogenation reaction on nickel–kieselguhr has been investigated at the conditions of the present experiment by Kehoe and Butt[14], who correlated the kinetics by the form:

$$-r_B = \frac{k_i^0 K^0 \exp[(-Q-E)/RT] P^2 x_B x_H}{1 + K^0 \exp(-Q/RT) P x_B} \tag{1}$$

The values of k_i^0, K^0, E and Q were redetermined in separate experiments for the batch of catalyst used in this study[13] using a differential reactor under the same conditions given in Table 1. Rate parameters were determined in two series of experiments corresponding to limiting forms of eqn (1). The first was at low temperature and high benzene concentration where:

$$-r_B \approx P x_H k_i^0 \,e^{-E/RT} = P x_H \cdot k_1(T)$$

and the second at high temperature and low benzene concentration, where:

$$-r_B \approx P^2 x_B x_H \,e^{(-Q-E)/RT} = P x_B x_H \cdot k_2(T).$$

These experimental data are shown in Fig. 2 and the results obtained by nonlinear least squares fit are summarized in Table 2.

Poisoning kinetics

Kinetics of the poisoning reaction were also determined in separate experimentation. The analysis of deactivation rates was carried out based on a separable[15] form of rate equation, linear in concentration of poison and availability of active sites. Thus:

$$-r_d = k_d^0 \,e^{-E_D/RT} P x_T \theta_A \tag{2}$$

and

$$k^0 = k_i^0 \theta_A \tag{3}$$

where θ_A is the ratio of the number of active sites to that under initial conditions and k^0 is the rate constant to be used in place of k_i^0 in eqn (1) as the catalyst deactivates. A similar rate equation for poisoning has been used by Richardson[9] for sulfur poisoning of Ni-kieselguhr, and good agreement with eqn (2) was obtained in the present study for temperatures from 65 to 175°C and thiophene partial pressures from 0·037 to 0·19 torr. Experimental results are shown in Fig. 3 and the values determined for k_d^0 and E_d are given in Table 3. However, while our experimental results in this range were correlated by eqn (2), there is evidence from the fixed bed studies which we discuss subsequently that poisoning kinetics may be rather more complicated than this.

Fixed bed deactivation

A number of typical initial (steady state) temperature profiles are shown in Fig. 4. These demonstrate the

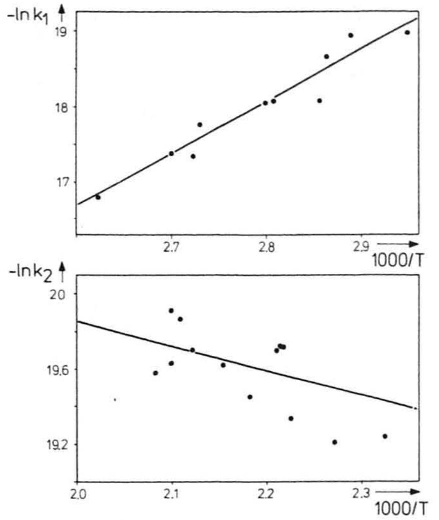

Fig. 2. Correlation of experimental data for benzene hydrogenation, eqn (1). $k^0 = k_i^0 e^{-E/RT}$; $K = K^0 e^{-Q/RT}$. Upper: T low, x_B high; $r_B \approx P x_H \cdot k_1(T)$; Lower: T high, x_B low; $r_B \approx P^2 x_B x_H \cdot k_2(T)$.

Table 2. Parameters for benzene hydrogenation kinetics

E	=	13,770 kcal/kmole
k_i^0	=	4.22 kmole/kg-sec-torr
Q	=	-16,470 kcal/kmole
K^0	=	4.22×10^{-11} torr^{-1}

Table 3. Parameters for thiophene poisoning kinetcs

E_d	=	1080 kcal/kmole
k_d^0	=	2.40×10^{-2} (torr-sec)$^{-1}$

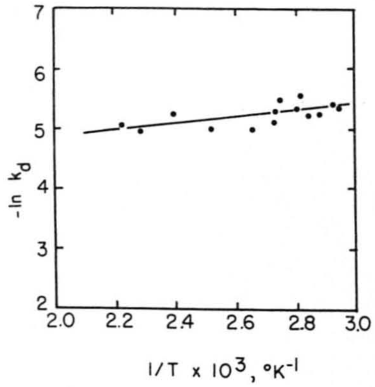

Fig. 3. Correlation of experimental data for thiophene poisoning, eqn (2).

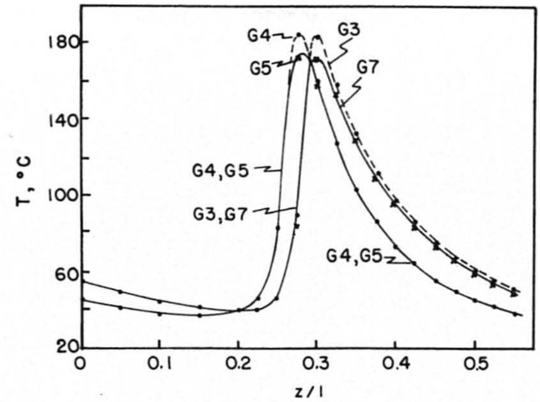

Fig. 4. Reproducibility of experimental temperature and conversion measurements.

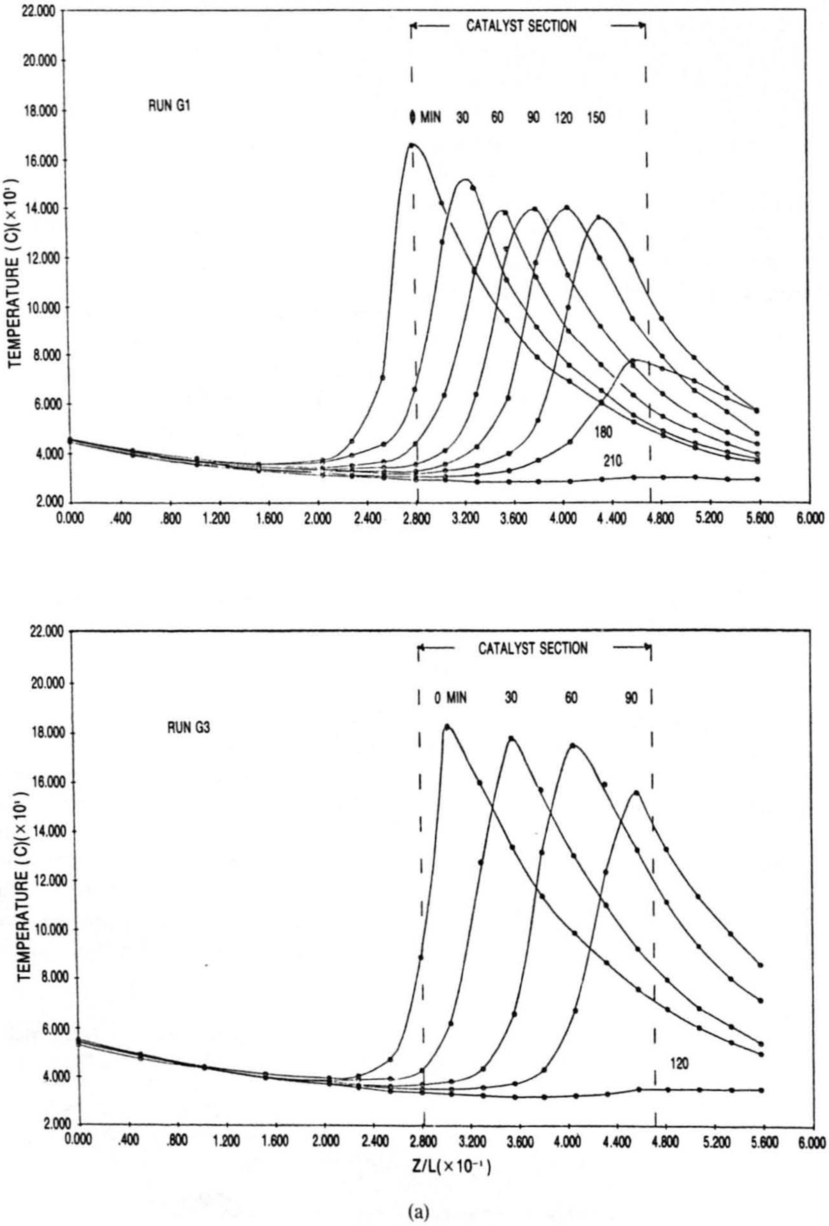

(a)

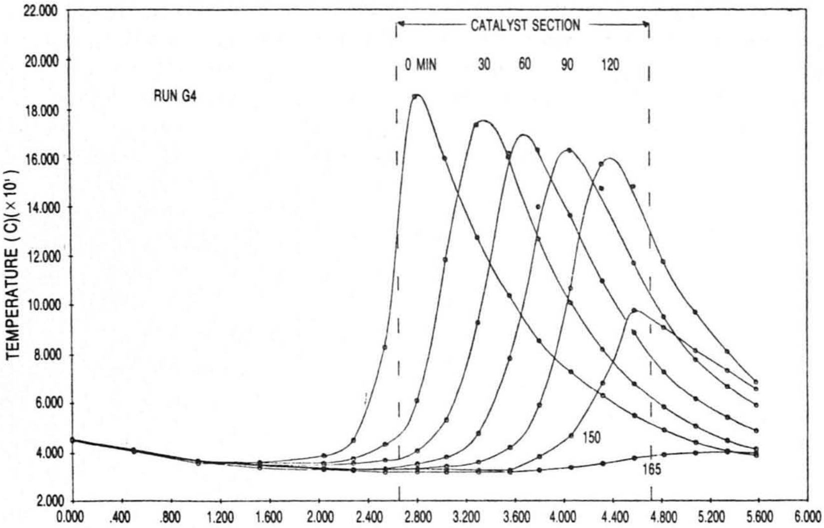

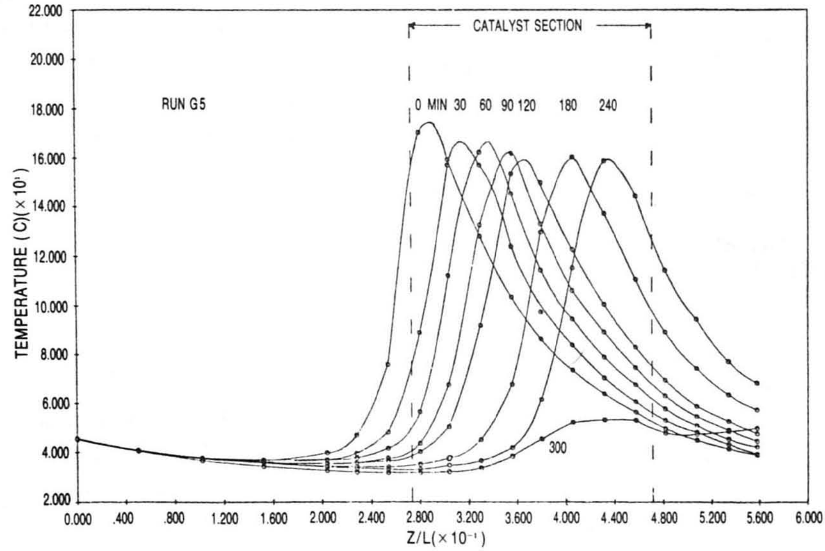

(b)

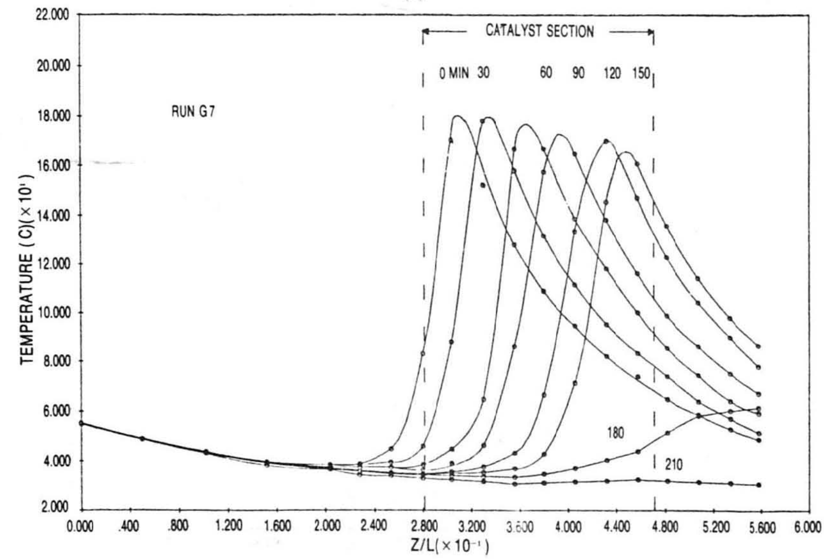

(c)

Fig. 5. Experimental temperature profile transients, Runs G1-G7.

reproducibility of results for experiments at similar conditions. There are possible thermal conduction effects on the thermocouple measurements, however, since the temperature gradients along the axis are large. In a number of experiments the temperature at a given point was measured from opposite directions (i.e. both from the top and the bottom of the reactor); the maximum difference observed in any experiment was 5°C. Radial gradients were also smaller than this in all cases. As will be seen, errors of this magnitude do not appear important in the interpretation of poisoning dynamics.

The time dependent temperature profiles measured for the runs listed in Table 1, except G2†, are shown in Fig. 5, and corresponding exit conversions in Fig. 6. A two-fold range of inlet benzene and thiophene concentration and a 1·5 fold variation in space velocity is encompassed by these experiments.

The temperature profiles in all cases move down the bed at almost constant speed, becoming a little broader as the end of the bed is approached. On reaching the end of the bed the hot spot diminishes in magnitude and then disappears within a short time interval. In runs G3 and G4 the movement of the profiles is more rapid due to higher thiophene feed content, while the profiles of G5 are wider and the hot spots a bit larger in magnitude, the result of lower flow rate through the bed. From the conversions shown in Fig. 6 it is seen that, from initial operation until near the end of a run, there is 100% conversion in each case, with a rapid fall-off near the end of operation. On comparison with the corresponding temperature profiles, it is seen that there is an excellent correlation between the rapid decrease in conversion and the movement of the hot spot out of the reactor.

INTERPRETATION

Modeling the experimental system

In view of the small reactor diameter involved in all experiments, a one dimensional axial dispersion model was used to model the reactor dynamics. As has been shown by Froment[16] and Finlayson[17] such a model is capable of accounting for the influence of a parabolic radial temperature profile if the wall heat transfer coefficient is chosen properly. The model includes material balance equations for benzene and thiophene, an energy balance, and the rate equation for catalyst deactivation. Since hydrogen was present in great excess the hydrogen concentration was essentially constant and volume contraction is not important. Thus we have:

(1) Mass balance, benzene

$$\epsilon\frac{\partial C_B}{\partial t} = \epsilon D_B\frac{\partial^2 C_B}{\partial z^2} - \epsilon\frac{\partial v C_B}{\partial z} + \theta_A \rho_C r_B(C_B, T). \tag{4}$$

(2) Mass balance, thiophene

$$\epsilon\frac{\partial C_T}{\partial t} = \epsilon D_T\frac{\partial^2 C_T}{\partial z^2} - \epsilon\frac{\partial v C_T}{\partial z} + \rho_C r_T(C_T, T, \theta_A). \tag{5}$$

(3) Energy balance

$$\frac{\partial T}{\partial t} = \frac{\lambda_{\text{eff}}}{\rho C_p}\frac{\partial^2 T}{\partial z^2} - \epsilon v\frac{\rho_g C_{pg}}{\rho C_p}\frac{\partial T}{\partial z} + \frac{2\alpha}{R_r \rho C_p}(T_w - T) + \frac{\theta_A(-\Delta H_R)}{\rho C_p}\rho_C r_B(C_B, T). \tag{6}$$

(4) Activity decay

$$\frac{d\theta_A}{dt} = r_d(C_T, T, \theta_A)$$

or

$$r_T = M_T r_d. \tag{7}$$

The boundary conditions corresponding are, at entrance:

$$\left.\frac{dY_i}{dz}\right|_{z=0} = \frac{v}{D_i}(Y_{i(z=0)} - Y_{i_0}) \tag{8}$$

where Y_{i_0} = feed values of C_B, C_T and T, and at exit:

$$\left.\frac{dY_i}{dz}\right|_{z=l} = 0. \tag{9}$$

†Although the experimental conditions for G2 differed from those for G3 almost exactly the same results were obtained.

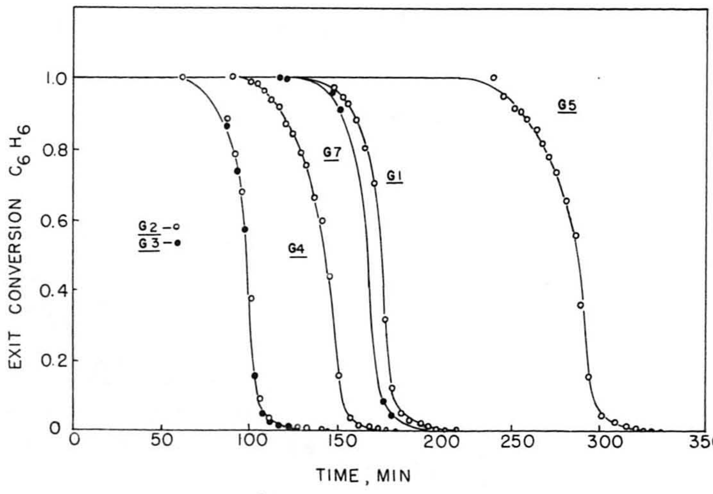

Fig. 6. Exit benzene conversion, all Runs.

The experimental configuration consisted of a packed catalyst section between fore and aft sections of inert glass beads, so that in solution of these equations the reaction rate terms and eqn (7) are not employed for the inert sections. Equations (4)–(6) make no mention of intraparticle or intraphase gradients, and in fact experimental conditions and reactor configuration were chosen in accordance with the criteria summarized by Mears and by Butt and Weekman[18] to ensure the absence of such gradients. Interphase temperature gradients are the most difficult to avoid in this system. Under the most extreme conditions in these experiments (i.e. at the location of the hot spot) the criterion developed by Mears for a less than 5% deviation in rate due to interphase temperature gradients requires a Nusselt number (hD_p/λ_g) of order 10. Our experimental values, according to the correlation of Littman *et al.*[19], are of order 5. Given the scatter in that correlation, we feel our conditions to be in order of magnitude agreement with the criterion of Mears, and the use of a pseudohomogeneous model justified.

Parameters

There are a number of parameters which appear in the model equations in addition to the kinetics. These have either been evaluated in separate experiments or, when reliable data or correlation exists, determined from the literature. Parameters are taken to be constant over the length of the reactor and with time of operation. The values employed are given in Table 4. Two of the parameters appearing in Table 4, M_T and α are particularly important in the modeling results and we shall give some detail on their determination here.

The thiophene capacity of the catalyst, M_T, is required to compute the thiophene mass balance, accounting for irreversible adsorption on the catalyst surface. This was measured by monitoring exit thiophene concentration from a fixed bed under reaction conditions from start up with fresh catalyst until complete deactivation was observed (no cyclohexane in product). Benzene and hydrogen at 0·835 and 585 cm^3/min(sc) were fed to a 2·5 cm dia. reactor containing 20·00 g of the reduced catalyst. Thiophene at a concentration of $5{\cdot}27\times 10^{-3}$ g/cm^3 in the benzene was introduced and exit thiophene concentration monitored with the result shown in Fig. 7. Complete deactivation was observed at 11·0 hr, with corresponding full break through of thiophene to its inlet concentration. Reaction zone temperature during this experiment was about 180°C. The amount adsorbed is determined as the difference in area between the two curves. On a relative basis $A_1/(A_1+A_2)$ is determined to be 0·597, thus:

$$M_T = (0{\cdot}597)(0{\cdot}835)(5{\cdot}27\times 10^{-3})(660)/20$$
$$= 1{\cdot}03\times 10^{-3}\ \text{kmole/kg catalyst.}$$

This corresponds to a value of $6{\cdot}2\times 10^{20}$ molecules/g catalyst. Based on an active Ni surface of approx. 24 m^2/g and unit stoichiometry for thiophene chemisorption per Ni atom, the number of adsorption sites is about 3×10^{15} cm^{-2}, a reasonable figure. For "five point" adsorption stoichiometry[22] the number is about 10^{16} cm^{-2}. It is important to note that this capacity was measured under reaction conditions, since Lyubarskii *et al.*[22] have shown significantly higher thiophene uptakes on Ni at temperatures above 100°C as compared to room temperature or slightly higher.

The second parameter, α, the wall heat transfer coefficient, was also determined experimentally, since there is a fair degree of uncertainty involved in using existing correlations, particularly for laboratory scale reactors. This was done using the measured temperature

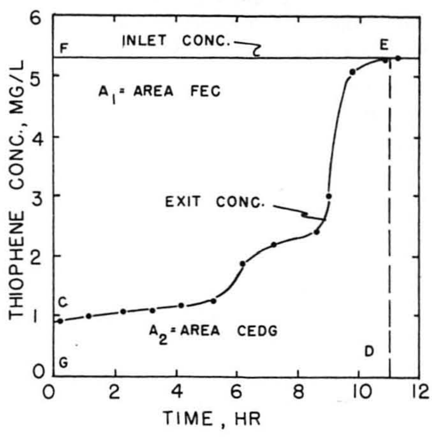

Fig. 7. Thiophene chemisorption under reaction conditions.

Table 4. Parametric quantities for modeling fixed bed deactivation of Ni hydrogenation catalyst by thiophene

Quantity	Evaluated from	Reference
Mol. Wt.	$MW = 2.106x_H + 78.12\ x_B$	——
ρ_g (kg/m^3)	$\rho_g = (MW)(273.16)P/(22.41)(760)T_o$	——
C_{pg} (350°K)$\left(\frac{\text{kcal}}{\text{kmole-°K}}\right)$	$C_{pg} = 6.935x_H + 23.15\ x_B$	API Tables
λ_{eff}(kcal/m-sec-°K)	$\lambda_{eff} = 7\lambda_g + 0.8\rho_g C_{pg} v\epsilon D_p$	
	$(\lambda_g \approx \lambda_{H_2})$	Yagi and Kuni [20]
D_T, D_B(m^2/sec)	$D_T = D_B = D_{C_6H_6/H_2} = 0.4\times 10^{-4}$ (45°C)	Krischer and Kröll [21]
α(kcal/m^2-°K)	$\alpha = 2.6\times 10^{-3}$	see text
ϵ	$\epsilon = 0.6$	Weng [13]
$\overline{\rho C_p}$ (kcal/m^3-°K)	$\overline{\rho C_p} \approx \bar{\rho}\cdot\overline{C_p} = 175$	——
M_T(kmole/kg)	$M_T = 1.03\times 10^{-3}$	see text

profiles in the inert fore and aft reactor sections determined at initial (steady state) conditions in the poisoning experiments. The analytical solution of the energy balance without reaction and at steady state

$$\lambda_{\text{eff}} \frac{d^2T}{dz^2} - v\rho_g C_{pg} \frac{dT}{dz} - \frac{2\alpha}{R_r}(T - T_w) = 0 \tag{10}$$

with B.C.: $T_{z=0} = T_0$, $T_{z=l} = T_L$ is:

$$T(z) = T_L \left[\frac{\exp p_2 z - \exp p_1 z}{\exp p_2 L - \exp p_1 L}\right] + T_0 \left[\frac{\exp(p_2 L + p_1 z) - \exp(p_1 L + p_2 z)}{\exp p_2 L - \exp p_1 L}\right] + \frac{\alpha_w}{\alpha_1}\left[1 + \frac{(\exp p_1 L - 1)\exp p_2 z - (\exp p_2 L - 1)\exp p_1 z}{\exp p_2 L - \exp p_1 L}\right] \tag{11}$$

where:

$$p_{1,2} = \frac{\bar{v}}{2\lambda_{\text{eff}}} \pm \left[\frac{\bar{v}^2}{2\lambda_{\text{eff}}^2} + \frac{\alpha_1}{\lambda_{\text{eff}}}\right]^{1/2}$$

$$\alpha_1 = \frac{2\alpha}{R_r};\quad \alpha_w = \frac{2\alpha}{R_r} T_w$$

$$\bar{v} = v\rho_g C_{pg}.$$

A nonlinear least squares analysis was used to fit the measured temperature profiles in the inert front and back sections. Since wall temperatures could not be reliably measured, values for T_w as well as λ_{eff} and α were estimated by this method. It was found that λ_{eff} was in good agreement with the correlation of Yagi and Kunii [19], so it was possible to fix λ_{eff} and estimate only α and T_w.

The most probable value for α ($2{\cdot}6 \times 10^{-3}$ kcal/m^2-sec-°K) was then used to determine the wall temperature giving best fit to experimental results. The wall temperatures so determined were somewhat higher than ambient, as shown in Table 5, but not greatly so. In modeling of the deactivation transients, an average of the T_w values obtained from the two inert sections was employed over the whole length of the reactor.

Computation of reactor dynamics

The system of eqns (4)–(9) was solved by a Crank–Nicholson method employing non-equidistant space steps and parabolic approximation of spatial difference quotients. Details of the procedure, which is generally applicable to diffusion models, will be reported elsewhere [23].

In Fig. 8 are shown results of the model calculations compared with experimental data on temperature profiles

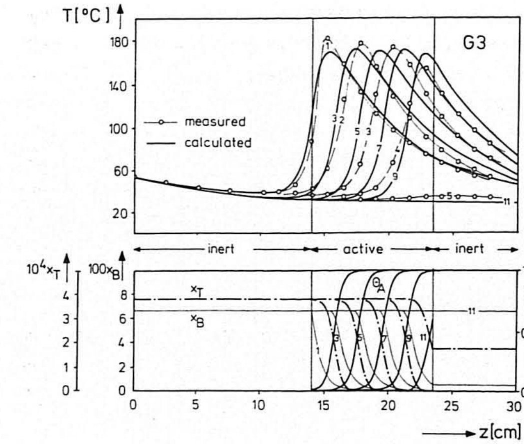

Fig. 8. Comparison of computed and experimental reactor dynamics for Run G3. Time marks: 1—steady state, $t = 0$; 2—$t = 30$ min; 3—$t = 60$ min; 4—$t = 90$ min; 5—$t = 120$ min; 6—$t = 150$ min; 7—$t = 180$ min; 8—$t = 210$ min; 9—$t = 240$ min; 10—$t = 270$ min; 11—$t = 300$ min.

from Run G3. The match to the initial steady-state profile is good, but that is the high point of the calculation. Clearly the calculated poisoning wave and corresponding hot spot location move through the bed much more slowly than was experimentally observed. For the example shown in Fig. 8 the zone of main reaction was at the end of the bed after 1·5 hr, while the corresponding calculation indicated 4 hr for this to occur.

These results are typical of the fit obtained with this model to all runs; calculated profiles pass through the bed more slowly than those measured experimentally, typically with a velocity of about 0·4 of the experimental value. There are two possible explanations for this:

(1) The calculation was found to be sensitive to the value of M_T, the total adsorption capacity for thiophene. If M_T is set at 0·4 of the experimentally determined value, the calculation gives a good correlation between theory and experiment for all the poisoning runs. However, while we can envision several reasons why the adsorption capacity experiment might have resulted in too small a value for M_T (bypassing, thermal desorption effects, reaction of thiophene), it is difficult to see how that experiment could overestimate M_T. The magnitude of experimental error in thiophene concentration measurement with the isatin–sulfuric acid method is much below that required to explain a two-fold discrepancy.

(2) The kinetic model for catalyst poisoning, eqn (12), may be inadequate and, in fact, there is some chemical evidence for this possibility. Lyubarskii *et al.* [22] and Berg *et al.* [24] have reported for thiophene on nickel, and Maxted [25] for thiophene on a number of transition metals, that their hydrogenation activity is not linearly

Table 5. Reactor wall temperatures

Run	G1	G2	G3	G4	G5	G7
Ambient Temperature, °C	19.0	23.0	22.0	23.0	23.0	22.0
T_w, Fore Section, °C	32.0	33.0	35.0	33.0	33.0	32.0
T_w, Aft Section, °C	27.5	25.0	23.0	25.0	25.0	23.0
$\bar{T}_w$, °C	29.7	29.0	29.0	29.0	29.0	27.5

related to the amount of poison on the surface. At lower loadings there is a large decrease in activity for small changes in loading, but at high values of loading the activity becomes independent of the amount of poison on the surface. In this case the adsorption capacity, M_T, as measured includes sites both active and inactive (or nearly so) for the hydrogenation reaction. The poisoning kinetics may then be treated to a much better approximation as shown below.

A two site model for thiophene chemisorption

If we consider the sites active for thiophene chemisorption to be the sum of those also active for hydrogenation and those active for chemisorption alone, the following balance equations may be written. For active sites:

$$\frac{d\theta_A}{dt} = r_d = -k_d^0 P x_T \theta_A \, e^{-E_d/RT} \qquad (12)$$

which is identical to eqns (2), (7) but where θ_A is defined as the ratio of hydrogenation active sites to the initial number of those sites. Since the kinetic parameters k_d^0 and E_d were measured experimentally by direct observation of the deactivation of the catalyst, they have the values given in Table 3. Now, for sites inactive in hydrogenation:

$$\frac{d\theta_I}{dt} = -k_{dI}^0 P x_T \theta_I \, e^{-E_{dI}/RT} \qquad (13)$$

where θ_I is the fractional occupancy of sites active only for thiophene chemisorption. If the activation energies E_d and E_{dI} are about equal and the rate constants differ in magnidude such that $k_{dI}^0 = f k_d^0$ $(0 < f < 1$, for preferential adsorption on hydrogenation active sites), the following relationship between θ_A and θ_I is established:

$$\theta_I = \theta_A^f \qquad (14)$$

the total rate of chemisorption of thiophene in this case is:

$$-r_T = P x_T M_T k_d^0 \, e^{-E_d/RT} \{\gamma \theta_A + f(1-\gamma)\theta_A^f\} \qquad (15)$$

where γ is the ratio of hydrogenation active sites to the total number obtained from measurement of M_T. If the constraint on $E_d \approx E_{dI}$ is not satisfied, then eqns (12) and (13) must be used together to obtain r_T. In the present instance, these activation energies appear small (if not equal) so the relationship of eqn (14) is reasonable. Thus, the only change required to use the two site model in the computation is the substitution of eqn (15) for eqn (7).

Discussion of results

Using either the original model, with an M_T of 0·4 the experimental value, or the two site model with the single set of parameters $f = 0{\cdot}015$ and $\gamma = 0{\cdot}35$, we have found it possible to obtain reasonable fits, essentially the same for both models, to all the experimental runs. Representative computed results are shown in Figs. 9–12 for Runs G3 to G7, both for the theoretical–experimental match on temperature profiles and for the computed values of θ_A, x_B

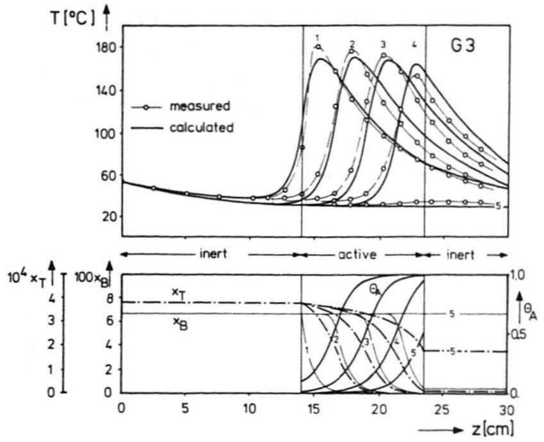

Fig. 9. Comparison of experimental temperature profile transients and calculated results from two-site deactivation model, Run G3. 1—$t = 0$; 2—$t = 30$ min; 3—$t = 60$ min; 4—$t = 90$ min; 5—$t = 120$ min.

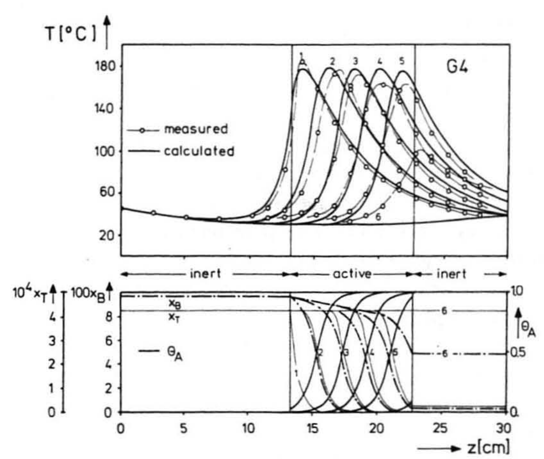

Fig. 10. Comparison of experimental temperature profile transitnts and calculated results from two-site deactivation model, Run G4. 1—$t = 0$; 2—$t = 30$ min; 3—$t = 60$ min; 4—$t = 90$ min; 5—$t = 120$ min; 6—$t = 150$ min.

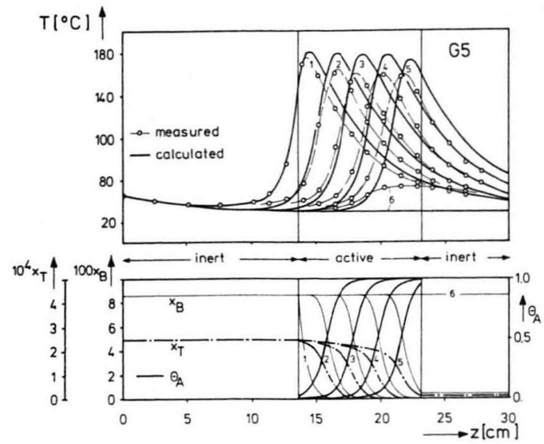

Fig. 11. Comparison of experimental temperature profile transients and calculated results from two-site deactivation model, Run G5. 1—$t = 0$; 2—$t = 60$ min; 3—$t = 120$ min; 4—$t = 180$ min; 5—$t = 240$ min; 6—$t = 300$ min.

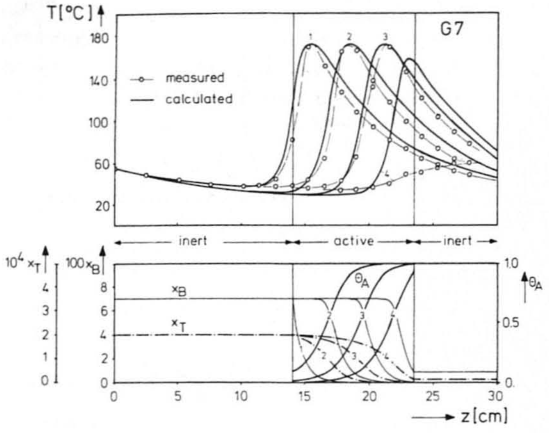

Fig. 12. Comparison of experimental temperature profile transients and calculated results from two-site deactivation model, Run G7. 1—$t = 0$; 2—$t = 60$ min; 3—$t = 120$ min; 4—$t = 180$ min.

and x_T through the reactor. The near-match between $\gamma = 0{\cdot}35$ in the two site model and the 0·4 factor on M_T required to force the single site model fit supports the plausibility of a two site chemisorption process in which 35–40% of total sites are active for the hydrogenation reaction. It should be noticed that while the activity and concentration gradients are rather sharp in most instances, corresponding to a moving active zone of about one-fifth the total catalyst bed, the thiophene and activity gradients in G3 and G7 extend through a large fraction of the bed length after initial operation. Thus, poison and activity "waves" may not be as sharp as the temperature gradients might lead one to expect.

In calculations with both models it was found that axial mass dispersion had only very small effects on the computed temperature profiles. An effective diffusivity for average experimental conditions, computed from a correlation such as that of Evans and Kenney[26], is $0{\cdot}35 \times 10^{-4}$ m²/sec, almost the same as the molecular diffusivity reported in Table 4. If desired, then, axial mass dispersion could be included in the models with an axial diffusivity of the same magnitude as the molecular diffusivity.

The calculated exit concentration of benzene is compared with experimental results in Fig. 13 for Run G5, which has about the porrest agreement between experiment and calculation of the series. The time of initial breakthrough of benzene from the reactor is very well predicted, although the calculation underestimates by about 10% the time required for complete deactivation of the bed. Also shown in Fig. 13 is the calculated thiophene concentration at the exit. This is qualitatively similar to the experimental results shown in Fig. 7 but a detailed comparison is not possible since no thiophene concentrations were measured in these runs.

The values of the parameters γ and f obtained in the fit with the two site model are reasonable in terms of their physical significance in the model. The f value indicates that thiophene chemisorption on the sites inactive for hydrogenation is slow compared to that on active sites, while the γ value indicates that there are somewhat fewer hydrogenation-active sites than inactive sites and as stated above this is in quantitative agreement with one site results. However, we cannot claim that this is a complete representation of the state of the catalyst surface without more detailed results on the intrinsic kinetics of thiophene poisoning of supported nickel.

CONCLUSIONS

While the present research has demonstrated agreement between reactor dynamics simulation and experiment, we have not yet attained the ultimate objective of complete, *a priori* prediction of dynamics due to poisoning using model parameters derived entirely from independent experimentation. A recurring theme is that poisoning kinetics in a reaction system such as this seem to be much more complex than the literature has generally given them credit for[1]. The entire question of linear poisoning models and of kinetic separability[15] between reaction processes and deactivation processes should be examined in detail, particularly for Langmuir–Hinshelwood rate correlations.

Acknowledgements—This research was supported by the National Science Foundation, GK-17200, by the Donors of the Petroleum Research Fund administered by the American Chemical Society, PRF-5087, and by the Deutsche Forschungsgemeinschaft. H-S. W. acknowledges partial fellowship support from the National Science Council, Republic of China.

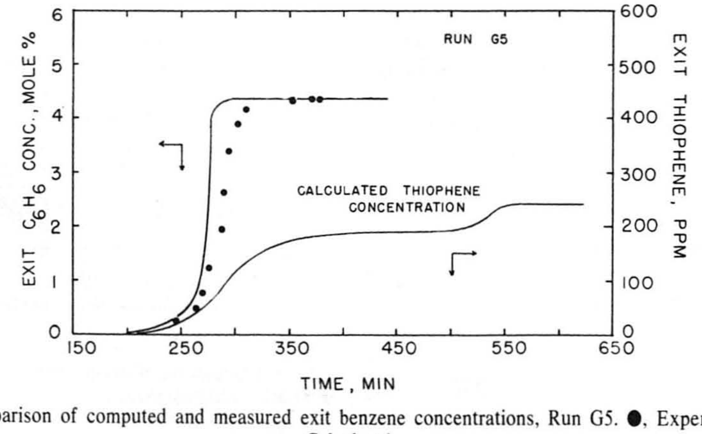

Fig. 13. Comparison of computed and measured exit benzene concentrations, Run G5. ●, Experimental; ——, Calculated.

NOTATION

C_B, C_T concentrations of benzene and thiophene, respectively (kmole/m^3)
C_{pg} heat capacity of the gas (kcal/kg-°K)
D_B, D_T molecular diffusivity of benzene and thiophene, respectively (m^2/sec)
D_p particle diameter (m)
E, E_d activation energies for hydrogenation and thiophene poisoning (kcal/kmole)
E_d, E_{dI} activation energies for two site poisoning model (kcal/kmole)
f ratio of pre-exponential factors for poisoning of inert of active sites
ΔH_R heat of benzene hydrogenation reaction (kcal/kmole)
k_i^0, k^0 rate constant for hydrogenation reaction on fresh and poisoned catalysts (kmole/kg-sec-torr)
k_d^0 pre-exponential factor for thiophene poisoning, one site model (torr-sec)$^{-1}$
k_{dA}^0, k_{dI}^0 pre-exponential factors for two site poisoning model, (kg/ksites-torr)
K^0 adsorption constant for benzene (torr)$^{-1}$
l reactor length (m)
M_T catalyst adsorption capacity for thiophene (kmole/kg)
P total pressure (torr)
$p_{1,2}$ constant appearing in eqn (11)
Q heat of adsorption parameter (kcal/kmole)
r_B, r_d rates of hydrogenation (kmole/kg-sec) and poisoning (θ_A/sec)
r_T rate of total thiophene chemisorption (kmole/kg-sec)
R gas constant (kcal/kmole-°K)
R_r reactor radius (m)
t time (sec)
T temperature (°K or °C)
$T_w, \bar{T}_w$ wall temperature and average wall temperature (°K or °C)
T_0, T_L inlet and outlet temperatures from inert reactor sections (°K or °C)
v interstitial velocity, m/sec
$\bar{v}$ constant appearing in eqn (11)
x_B, x_H, x_T mole fractions of benzene, hydrogen and thiophene
Y_i quantity defined in eqn (8)
z length variable (m)

Greek symbols

α wall heat transfer coefficient (kcal/m^2-°K)
α_1 constant appearing in eqn (11)
α_w constant appearing in eqn (11)
γ ratio of hydrogenation-active sites to total sites measured by M_T
ϵ bed void fraction
λ_{eff} bed effective thermal conductivity (kcal/m-sec-°K)
θ_A, θ_I fractional occupancy of hydrogenation-active and -inactive sites by thiophene
ρ_c, ρ_g catalyst and gas densities (kg/m^3)
ρC_p average volumetric heat capacity (kcal/m^3-°K)

REFERENCES

[1] Butt J. B., *Adv. Chem.* 1972 **109** 259.
[2] Eberly P. E., Jr., Kimberlin C. N., Miller W. H. and Drushel H. V., *Ind. Engng Chem. Proc. Design Devel.* 1966 **5** 193.
[3] Menon P. G. and Sreeramamurthy R., *J. Catal.* 1967 **8** 95.
[4] Menon P. G., Sreeramamurthy R. and Murti P. S., *Chem. Engng Sci.* 1972 **27** 647.
[5] Kungita E., Saga K. and Otake T., *J. chem. Engng Japan* 1969 **2** 75.
[6] Lambrecht G. C., Nussy C. and Froment G. F., *5th European Symp. on Chem. Reaction Engng* B2–19, Elsevier, Amsterdam, 1972.
[7] Froment G. F. and Bischoff K. B., *Chem. Engng. Sci.* 1961 **16** 189.
[8] Pexidr V., Cerny J. and Pasek J., *4th European Symp. on Chem. Reaction Engng* p. 239. Pergamon Press, Oxford, 1970.
[9] Richardson J. T., *J. Catal.* 1971 **21** 130.
[10] Bohart G. and Adams E., *J. Am. Chem. Soc.* 1920 **42** 523.
[11] Irving J. P. and Butt J. B., *Chem. Engng Sci.* 1967 **22** 1857.
[12] Kehoe J. P. G., Ph.D. Dissertation, Yale University. New Haven, Conn., 1971.
[13] Weng H. S., Ph.D. Dissertation, Northwestern University, Evanston, Ill., 1974. Available from University Microfilms.
[14] Kehoe J. P. G. and Butt J. B., *J. appl. Chem. Biotechnol.* 1972 **23** 22.
[15] Szepe S. and Levenspiel O., *4th European Symp. on Chem. Reaction Engng* p. 265, Pergamon Press, Oxford, 1970.
[16] Froment G. F., *Ind. Engng Chem.* 1967 **59** 18.
[17] Finlayson B. A., *The Method of Weighted Residuals and Variational Principles*, p. 131. Acedmic Press, New York, 1972.
[18] Butt J. B. and Weekman V. W., Jr., *CEP Symp. Series* 143. 1974; **70** 27 Mears, D. E., *Ind. Engng Chem. Proc. Des. Develop.* 1971 **10** 541.
[19] Littman H., Barile R. G. and Pulsifer A. H., *Ind. Engng Chem. Proc. Des. Develop.* 1971 **10** 541.
[20] Yagi, S. and Kuni D., *A. I. Ch. E. Jl.* 1957 **3** 373.
[21] Krischer O. and Kroll K., *Die wissenschaftlichen Grundlagen der Trocknungstechnik*, p. 176, Springer-Verlag, Berlin, 1963.
[22] Lyubarskii G. D., Andeeva L. B. and Kul'kova N. V., *Kin. i Kat.* 1962 **3** 123.
[23] Eigenberger G. and Butt J. B., *A Crank-Nicholson Method with Non-equidstant Space Steps*, to be published.
[24] Berg G. A., Sokolova, V. I. and Masagutov R. M., *Tr. Bashkir. Nauk. Issled, Inst. Pererab. Nefti.* 1968 **8** 115.
[25] Maxted E. B., *Adv. Catalysis* 1951 **3** 129.
[26] Evans E. V. and Kenney C. N., *Trans. Instn. Chem. Engrs.* 1966 **44** T189.